

Effect of Bubble Influence Area Factor on Wall Heat Flux Partitioning in CUPID Simulation of SUBO Experiment

Y. J. Cho^{a*}, H. Y. Yoon^a

^aKorea Atomic Energy Research Institute, 111 Daedeok-daero, 989 Beon-gil, Yuseong-gu, Daejeon 305-600

*Corresponding author: yjcho@kaeri.re.kr

1. Introduction

Since the heat flux partitioning model had been suggested by Kurul and Podowski [1], it has been widely used in various commercial and in-house CMFD codes [2, 3]. The heat flux partitioning model consists many sub-models such as the heat transfer coefficient of single-phase convection, heat transfer coefficient of quenching effect, bubble departure diameter, bubble departure frequency, nucleation site density, and so on. Thus, the heat flux partitioning and the boiling behavior can be changed by the selection of sub-models. This fact means that it is very important to select proper sub-models by considering the thermal-hydraulic conditions of target problem.

Various sensitivity calculations were performed with varying the sub-models in the heat flux partitioning model so far. However, the bubble influence area factor (K) was usually assumed as a constant in their researches even though it can play an important role in determining not only the initiation of the subcooled boiling and the heat flux partitioning itself.

In this study, the literatures on the bubble influence area were reviewed and its effect on the simulation of subcooled boiling using CUPID code was evaluated.

2. Bubble Influence Area Factor

2.1 Importance of Bubble Influence Area Factor

The bubble influence area factor is one of important constitutive model for closure of the heat flux partitioning equation. This factor is used for calculation of the heat transfer areas for the both of single phase convection and boiling heat transfer so that it plays an important role for partitioning of heat flux from walls. In addition, the bubble influence area factor affect the onset of nucleate boiling (ONB) point in high subcooled region as well as the maximum vapor generation rate in low subcooled region. Nevertheless, the bubble influence factor has been used as a constant from 1.8 to 4.0 without any proper model or correlation that can represent the dependency of the factor on thermal-hydraulic parameters.

2.2 Literature Review

Hsu [4, 5] observed the deactivation of adjacent nucleation sites within the influence area of a boiling bubble and reported that the area of influence of each bubble was roughly twice of the bubble radii. Gaetner [6]

experimentally supported Hsu's result with the plating technique. Han [7] also experimentally observed that the radii of influence area is twice of the bubble radii by the demonstration with chalk powder and a solid ball.

After these studies, many researchers used the bubble influence factor as a constant from 1.8 to 4.0. In particular, the constant value of 4 is the most frequently used value by Mikic [8], Krepper [9], Koncar [10], and so on.

In some studies, the bubble influence area factor was calculated from the experimental data. Judd [11] fitted the bubble influence area factor from the experimental data and suggested the constant value of 1.8. Valle [12] calculated the bubble influence factor from the energy balance equation and reported the constant value from 5.8 to 7.5 according to the test cases.

Recently, the direct measurement of local wall temperature was performed in several studies as the measurement technique has been developed. The results of the direct measurement were incompatible with the earlier observation results by Hsu, Gaetner, and Han. The earlier results showed the bubble influence area factor is larger than 1.8. On the other hand, the bubble influence area factor is generally smaller than 1.0 in the direct measurement results.

Kenning [13] suggested that the bubble influence factor is almost 1.0 in the experiment by using a liquid crystal thermography. Demiray [14] measured the local heat flux and wall temperature by 96 of platinum heater arrays and reported that the bubble influence area factor is around 0.25. Sanna [15] also measured the local wall temperature by using the heater array similar with Demiray and reported that the value is about 0.25. Golobic [16] measured the local wall temperature during the bubble life cycle by using an IR thermometer. He also reported that the bubble influence area factor is smaller than 1.0.

From the result of literature review, we can notice that the recent measurement results significantly differ from the earlier research results. It is not easy to say which result is correct or not. However, it is clear that the effect of the bubble influence area factor should be investigated especially for the case where the bubble influence area factor of 1.0 or less is adopted in CMFD calculations.

3. CUPID Simulation of SUBO Experiment

3.1 SUBO Experiment [17]

SUBO experiment was performed to investigate the subcooled boiling phenomena by measuring the local bubble parameters. The local void fraction, the bubble velocity, the Sauter mean diameter and the interfacial area concentration were measured by using a double sensor optical fiber probe in order to quantify the complicated bubble behavior in a two-phase flow condition.

Six tests were performed varying the heat flux, the inlet mass flux and the inlet temperature while the outlet pressure was kept at 160 kPa. In this study, the base case was selected for the sensitivity calculation. The heat flux, inlet mass flux, inlet temperature, and outlet pressure for the base case are 473.7 kW/m², 1124.7 kg/m²s, 374.65 K, and 161.6 kPa, respectively.

3.2 Grid Generation

The test section of SUBO is vertical annulus with an indirect heater rod at the center of the channel as shown in Fig. 1. (a). In the CUPID calculation, the heated section and the bubble condensation region above the heated section are modeled as shown in Fig. 1. (b). Two dimensional mesh with a fan-shape base area was generated because the test section is symmetry in azimuthal direction. 12x1x100 grids were used for r- θ -z coordinates.

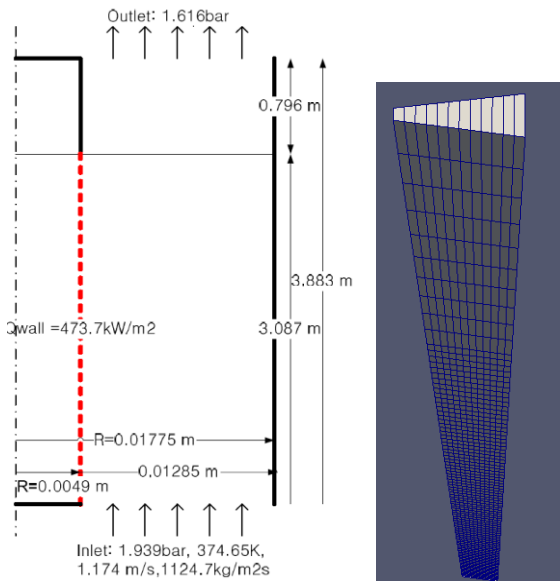


Fig. 1. Calculation domain for SUBO test: (a) Schematic Diagram (b) Mesh

3.3 Heat Flux Partitioning Model in CUPID

CUPID code adopt the heat flux partitioning model for analyzing the wall boiling including the sub-cooling boiling in computational mesh cells facing a heated wall. In the model, the heat transfer from the heated wall surface to the fluid is expressed as a sum of surface quenching heat transfer, wall boiling heat transfer and

heat transfers to each phase as shown in Eq. (1) ~ Eq. (4). The bubble influence area factor (K) is used for calculating the single- and two-phase heat transfer area fractions as shown in Eq. (5).

$$Q_{wall} = Q_q + Q_e + Q_c \quad (1)$$

$$Q_q = h_q A_{2f} (T_w - T_l) \quad (2)$$

$$Q_e = N'' f \left(\frac{\pi}{6} D_{b,depart}^3 \right) \rho_g h_{fg} \quad (3)$$

$$Q_c = h_{c,l} (1 - A_{2f}) (T_w - T_l) \quad (4)$$

$$A_{2f} = N'' \frac{\pi D_{b,depart}^2}{4} K \quad (5)$$

Where Q_{wall} , Q_q , Q_e , Q_c , h_q , A_{2f} , T_w , T_l , N'' , f , $D_{b,depart}$ and $h_{c,l}$ are total wall heat flux, quenching heat flux, evaporation heat flux, single-phase convection heat transfer coefficient, two-phase heat transfer area fraction, wall temperature, liquid temperature, nucleate site density, bubble departure frequency, departure bubble diameter, and single phase heat transfer coefficient, respectively.

The two-phase heat transfer area fraction (A_{2f}) cannot exceed 1.0 due to the definition of the fraction. Therefore, the maximum value of the nucleate site density also can be derived from Eq. (1) when the two-phase heat transfer area fraction is equal to 1.0.

4. CUPID1.8 Calculation

4.1 Sensitivity Test for Bubble Influence Area Factor

The CUPID calculations were performed with 3 different bubble influence area factors of 1.0, 2.0 and 4.0. As shown in Fig. 2 ~ Fig. 4, the radial and axial distributions of void fraction are significantly changed with varying the bubble influence area factor. As mentioned in Section 2.1, the bubble influence area factor affect the ONB point because the single phase heat transfer increases if the bubble influence area factor become smaller. So, the ONB point is delayed as the bubble influence area factor decreases.

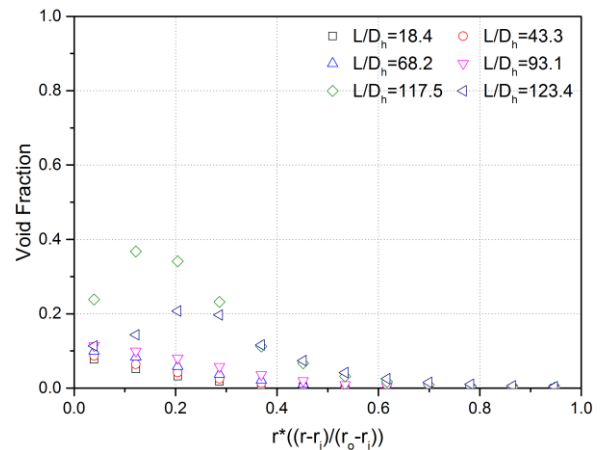


Fig. 2. Calculation result of void fraction distribution ($K=4.0$)

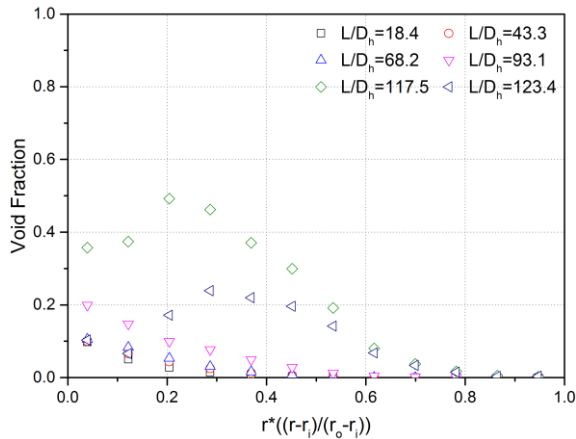


Fig. 3. Calculation result of void fraction distribution ($K=2.0$)

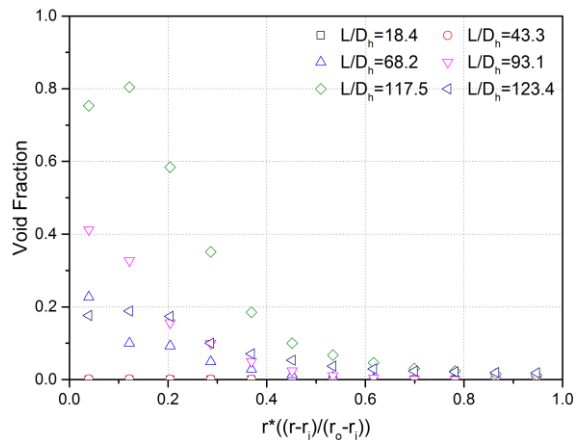


Fig. 4. Calculation result of void fraction distribution ($K=1.0$)

On the other hand, the void fraction at the higher height where the local subcooled is relatively low increases as the bubble influence area factor decreases. The calculation equation of the maximum nucleate site density in Eq. (5) is responsible for the result.

4.2 Other Effective Parameters on ONB Point

Although the ONB point is varied by the bubble influence area factor, it is obvious that there are other effective parameters on the ONB. For example, the ONB can occur at the low height if the boiling induced turbulence model is turned off due to the decreased of thermal mixing between the subcooled liquid region and the core region of the channel. On the other hand, the ONB point is delayed if the nucleation site density model is changed to generate the site density at higher wall superheat. Fig. 5 shows the effect of the boiling induced turbulence model and the nucleation site density model described above. In CUPID, Lahey's bubble induced turbulence model [18] was used. The nucleation site density model was changed from Cole's model [19] to Hibiki's model [20] for this sensitivity test.

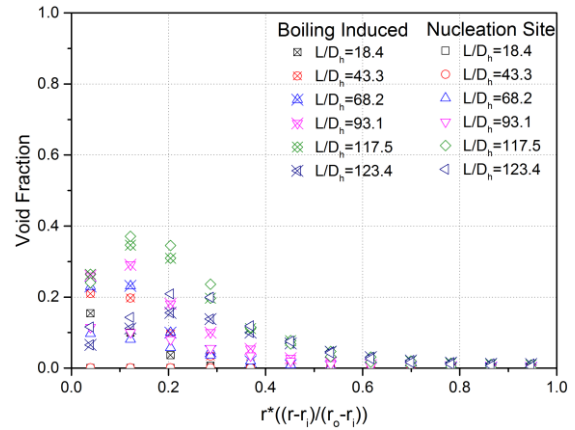


Fig. 5. Calculation result of void fraction distribution with different boiling induced turbulence model and nucleation site density model ($K=4.0$)

5. Conclusions

Nevertheless many of recent research results showed that the bubble influence area factor does not exceed 1.0, most of CMFD calculations have been performed by assuming the bubble influence area factor is larger than 1.0. The most frequently used value was 4.0.

In this paper, the effect of the bubble influence area factor was evaluated on the ONB point and the maximum nucleation site density, which determines the maximum vapor generation rate. If the bubble influence area factor was reduced from 4.0 to 1.0, the ONB was delayed and the vapor generation rate in the low subcooled region increased. Even though there are other effective parameters as shown in Section 4.2, this result can be a useful guide when one is willing to perform the sensitivity calculation with different models in the heat flux partitioning equation especially in the case where the fixed constant value is used for the bubble influence area factor.

ACKNOWLEDGMENTS

This work was supported by National Research Foundation of Korea (NRF) grant funded by the Korea government (MSIP).

REFERENCES

- [1] N. Kurul, M. Z. Podowski, On the modeling of multidimensional effects in boiling channels, ANS Proceedings of 27th National Heat Transfer Conference, Minneapolis, MN, 1991.
- [2] CD-adpco, STAR-CCM+ User Guide, 2006.
- [3] Y. Egorov, F. Menter, Experimental Implementation of the RPI Wall Boiling Model in CFX-11. Ansys Cfx, Staudenfeldweg 12, 83624 Otterfing, Germany, 2004.
- [4] Y. Y. Hsu, Gradual Transition of nucleate boiling from discrete-bubble regime to multi bubble regime, NASA TN D-2564, National Aeronautics and Space Administration, 1964.
- [5] Y. Y. Hsu, R. W. Graham, An analytical and experimental study of the thermal boundary layer and ebullition cycle in

nucleate boiling, NASA TN D-594, National Aeronautics and Space Administration, 1961.

[6] R. F. Gaertner, Photographic study of nucleate pool boiling on a horizontal surface, Paper 63-WA-76, ASME, 1963.

[7] C. Y. Han, P. Griffith, The mechanism of heat transfer in nucleate pool boiling-part II, *Int. J. Heat Mass Transfer*, Vol. 8, pp. 905-914, 1965.

[8] B. B. Mikic, W. M. Rohsenow, A new correlation of pool-boiling data including the effect of heating surface characteristics, *J. Heat Transfer*, Vol. 91, pp. 245-250, 1969.

[9] E. Krepper, B. Koncar, Y. Egorov, "CFD modeling of subcooled boiling – Concept, validation and application to fuel assembly design," *NED*, Vol. 237, pp. 716-731, 2007.

[10] B. Koncar, I. Kljenak, B. Mavko, Modeling of local two-phase flow parameters in upward subcooled flow boiling at low pressure, *Int. J. Heat and Mass Transfer*, Vol. 47, pp. 1499-1513, 2004.

[11] R. L. Judd, K. S. Hwang, A comprehensive model for nucleate pool boiling heat transfer including microlayer evaporation, *J. Heat Transfer*, Vol. 98, pp. 623-629, 1976.

[12] Victor H. Del Valle M. and D. B. R. Kenning, Subcooled flow boiling at high heat flux, *Int. J. Heat Mass Transfer*, Vol. 28, pp. 1907, 1985.

[13] D.B.R. Kenning, Youyou Yan, Pool boiling heat transfer on a thin plate: features revealed by liquid crystal thermography, *Int. J. Heat Mass Transfer*, Vol. 39, No. 15, pp. 3117, 1995.

[14] F. Demiray, J. Kim, Microscale heat transfer measurements during pool boiling of FC-72: effect of subcooling, *Int. J. Heat Mass Transfer*, Vol. 47, pp. 3257, 2004.

[15] A. Sanna, et al., Numerical investigation of nucleate boiling heat transfer on thin substrates, *Int. J. Heat Mass Transfer*, Vol. 76, pp. 45, 2014.

[16] I. Golobic, et al. Experimental determination of transient wall temperature distributions close to growing vapor bubbles, *Int. J. Heat Mass Transfer*, Vol. 45, pp. 857, 2009.

[17] B. J. Yun, B. U. Bae, D. J. Euh, G. C. Park, C. -H. Song, Characteristics of the local bubble parameters of a subcooled boiling flow in an annulus," *Nuclear Engineering and Design*, Vol. 240, pp. 2295-2303, 2010.

[18] R. T. Lahey, The simulation of multidimensional multiphase flows, *Nuclear Engineering and Design*, Vol. 235, pp. 1043-1060, 2005.

[19] R. Cole and W. Rohsenow, Correlation of bubble departure diameters for boiling of saturated liquids, *Chem. Eng. Prog. Symp. Ser. Vol.65 (92)*, pp.211-213. 1969.

[20] T. Hibiki, M. Ishii, Active nucleation site density in boiling system, *Int. J. Heat and Mass Transfer*, Vol. 46, 2587-2601, 2003.